

## **Application of electrical resistivity method in delineating aquifer properties along with vulnerability mapping in Gujrat District and surrounding areas of Punjab province, Pakistan**

**Abrar Niaz<sup>1\*</sup>, Muhammad Rustam Khan<sup>1</sup>, Fahad Hameed<sup>1</sup>, Aamir Asghar<sup>3</sup>, Anees Ahmad Bangash<sup>4</sup>, Umair Bin Nisar<sup>2</sup>, Jawad Niaz<sup>1</sup> Muhammad Farooq<sup>1</sup>, Muhammad Yasin Khan<sup>1</sup> and Mansoor Awan<sup>1</sup>**

<sup>1</sup>*Institute of Geology, University of Azad Jammu & Kashmir, Muzaffarabad*

<sup>2</sup>*Comsats institute of information technology, Abbottabad*

<sup>3</sup>*Institute of Geology University of Poonch, Rawlakot Azad Jammu & Kashmir*

<sup>4</sup>*Quaid e Azam University, Islamabad*

*\*Corresponding author's email: abrar.niaz@ajku.edu.pk*

*Submitted: Dec 20, 2017 Accepted date: Oct 18, 2019 Published online:*

### **Abstract**

A resistivity investigation was directed to assure aquifer properties besides delineation of vulnerability in the Gujrat District and its surroundings areas of Punjab province, Pakistan using seventy-seven (77) Schlumberger array Vertical Electric Sounding (VES). The data was processed in IPI2WIN computer software for true resistivity and thickness of layers. The available borehole information demonstrates presence of best top clay, sandy clay, dry sandy soil and gravel. The prolific ground water zones (controlled by H-type resistivity curve) have been recognized in the north-eastern, southern and additionally western part of the study area. The thickness of aquifers fluctuates remarkably 20-210 m from place to place. The aquifer vulnerability map delineates the impermeability of overburden clay layer. Values < 0 mhos show poor to weak protective capacity zone with risk of defilements, while 0-5 mhos demonstrates good protective zones. The outcomes were additionally checked by anisotropy mapping and chemical investigation of well's water samples of the study area. The outcomes of anisotropy values show that Nither town and southern halves of the study area have a good protective capacity to infiltration while remaining area is vulnerable to infiltrating fluids. The water from this area is found polluted with chlorides, nitrates and sulphates salts.

*Keywords:* Groundwater potential, Anisotropy mapping, Vertical Electrical Sounding (VES), Vulnerability mapping, Chemical investigation.

### **1. Introduction**

The Potwar basin straddles District Gujrat, province of Punjab, Pakistan. The area possesses monotonous view in all directions. The native residents have confronted springs of resentments of water scarcity in the area. Thus, there is a need to disclose new ground water assets or to draw more ground water to the surface using systematic hydrological investigation in the region in order to provide freshwater to the local inhabitants. The geophysical techniques are effective for data acquisition of Quaternary deposits, while electric resistivity technique was regularly employed in the assurance of ground water potential, quality variety, isolation of subsurface strata and any susceptibility of aquifer to contaminants (Kenneth and Edirin, 2012). Similarly, VES and imaging have

portrayed ground water vulnerability (Ogunbe et al., 2012), hence perceptible for hydro-geological analysis of Geological Formations (Kelly and Stanislav, 1993).

The geophysical method for resistivity was used to determine apparent resistivity of rock and soil at profundity or at immediate location. The technique allow to construct an hydrogeological model of the investigated area (Awni, 2010; Bayewu et al., 2014). The electrodes are coerced in straight paths for different configurations (dipole-dipole, Schlumberger and Wenner pattern). The current is being governed by the apparent resistivity of rocks and soil. The apparent resistivity is computed by rationing the calculated resting potential with inserted current and multiplying geometric component peculiar to the pattern in use and electrode position (Stanley and Davis, 1996).

The electrodes spacing from any particular distance of fixation is equitably extended for inward penetrations (Adeoti et al., 2012; Gowd, 2004) and resistivity's fluctuations with profundity are plotted on the converse and onward patterned computer software. The Vertical Electric Sounding (VES) technique was employed as it possesses common instruments, easy to operate in field and straight forward data examination (Zohdy et al., 1974; Stampolidis, et al., 2005; Soupios, et al., 2007; Kalisperi, et al., 2009). The procedure was already used to estimate perpendicular variation of electric resistivity (Anomohanran, 2013). Moreover, the VES lacks any repetition and sparing of information (Madan et al., 2008; Ako and Olorunfemi, 1989). It is used in differentiating saturated layers from unsaturated.

The Schlumberger pattern possesses a considerable depth of penetration as compared to the Wenner arrangement. In resistivity technique, Wenner array is utilized for the shallow depth, while Schlumberger arrangement is utilized for deeper soundings (Olowofela et al., 2005). Geoelectric technique is frequently used for the demarcation of profundity, breadth and perimeters of aquifers (Omosuyi et al., 2007). The aquifer's resistivity and thickness are utilized for computation of transverse resistance and in compiling perpendicular conductance (Ekwe et al., 2010). It is likewise utilized as a part of assurance of groundwater probability (Oseji et al., 2005), investigation of geothermal reservoirs and estimation of hydraulic potential of ground water (El-Qady, 2006). Vanderborgh et al., (2005) and Kemna et al., (2002) employed inverse conductivity modelling for demarcation of solute plumes. Conductivity 2D converse modelling was executed for the investigation of solute plumes. The resistivity technique was employed for determination of groundwater potential and contamination assessment (Niaz et al., 2017; Niaz et al 2013). The conjugate techniques resistivity and petrographic analysis were also found promising in groundwater profile identification (Niaz et al., 2018). Nisar et al., (2018), delineated Ground water occurrence in relation with quaternary paleo-depositional environments.

The present study aims at determining the groundwater potential zones and vulnerability risk assessment in the area using geoelectric and chemical analysis methods in Gujrat district and its surroundings areas.

## 2. Geological frame work of the area

Study area forms broad, active, sedimentary basin known as Potwar basin and exists in Punjab province of Pakistan. The area comprises Himalayan molasse sediments and includes inundated stream and flood plain deposits, terrigenous sedimentary rocks and older terrace sediments. These deposits form clay, sandy clay, dry sandy soil, gravels and boulders (Fig. 1; Shah, 1977 and Shah, 2009). The molasse deposits comprises of two main groups, Rawalpindi group and Siwalik group of rocks. The Rawalpindi group (Miocene age) is further categorized in Murree Formation and Kamliyal Formation. The Murree Formation consist of cyclic deposition of clay and sandstone whereas, Kamliyal Formation dominantly consist of sandstone. The Siwalik group (Pleistocene age) of rocks comprises of four formations namely Chinji Formation, (70 % clays and 30 percent friable sandstone), Nagri formation (30 % clay and 70 % sandstone), Dhok Pathan Formation (50 % clay and 50 % sandstone) and Soan Formation (recent deposits and conglomerate) (Shah, 2009). The litho-logs of drilled wells in this area computed with interpreted model and calibrate the obtained results. The recent alluvium deposits are also present as top cover. These deposits comprises of patches clay, sand, silt, gravels and boulders.

### 2.1. Hydrogeological setting of the study area

The research area includes the terrigenous sedimentary rocks of stream deposits, flood plain deposits, detrital sedimentary rocks and Siwalik group of rocks. These sediments co-exist in different proportions and alternate from sandy clay to clayey sand. The sand, gravel and their admixtures serve as water bearing strata, hence, relatively enduring in terms of water production. The Siwalik Group of rock formation is also present in this area. The sandstone of these formation is soft in nature and suitable for water storing whereas, clays act

as a barriers for groundwater storage in the subsurface. Most of the aquifers in this region are confined however some places are characterized by unconfined aquifers with gravels and boulders at the top. Moreover, the aquifers are recharged by the effective infiltrations and seasonal tributaries draining the area. The yearly rainfall of around 1033 mm (climate-data.org) has been recorded in the area. The Jhelum River is also running in north

western part of the area. Some canals from Jhelum river are also flowing in the area. The river, canals and seasonal drainage are the main source of recharging subsurface aquifers. The heat of the sun lingers at evening time during summer. The water table in the area is fluctuating depending upon seasonal recharging.

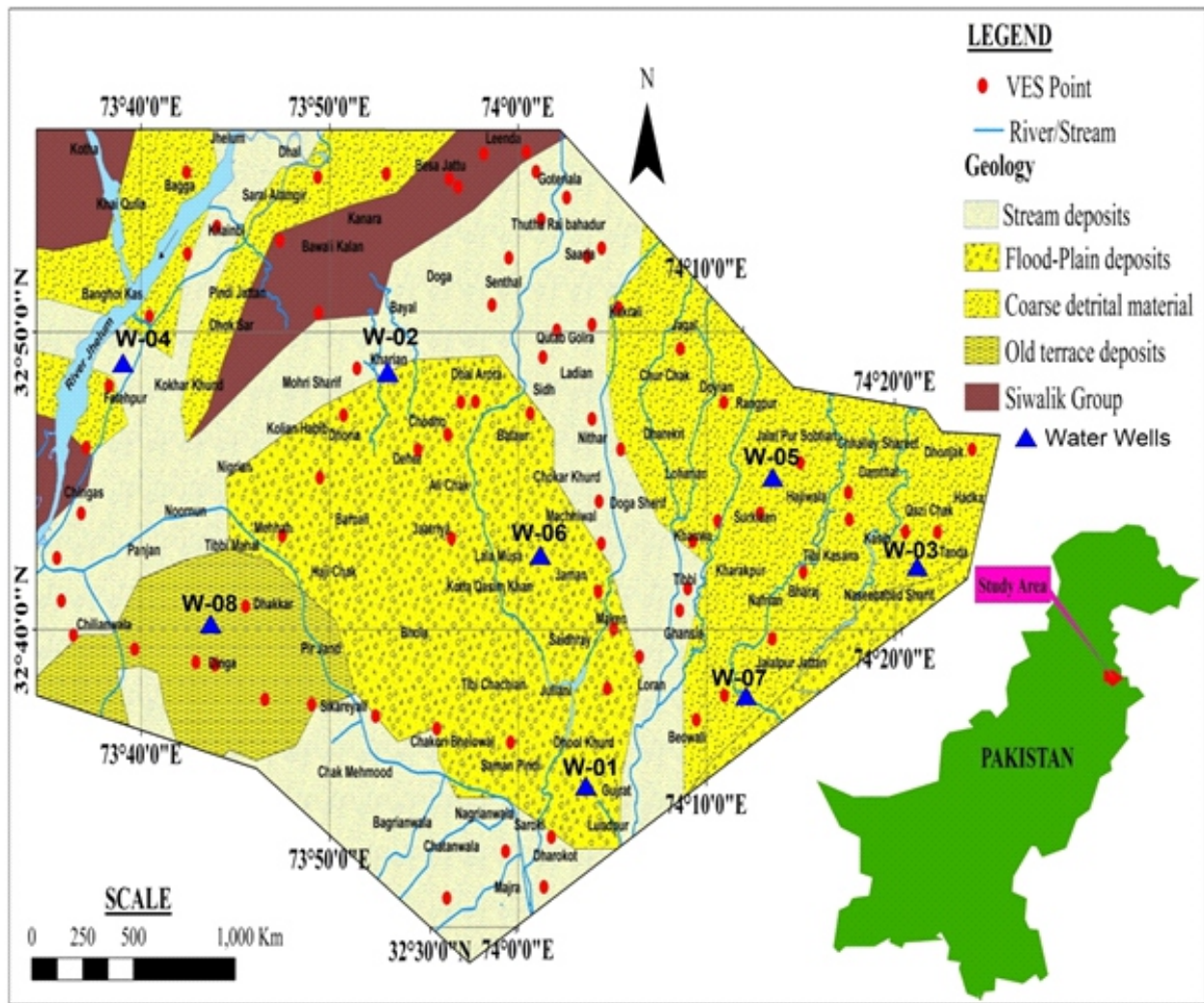


Fig. 1. Geological and location map of study area.

Table 1: Modified longitudinal conductance/protective capacity rating (Henriet, 1976).

Longitudinal conductance (mhos)	Protective capacity rating
>10	Excellent
5 – 10	Very good
0.7 - 4.9	Good
0.2 - 0.69	Moderate
0.1 - 0.19	Weak
<0.1	Poor

### 3. Materials and methods

The Schlumberger configuration was used in systematic hydrologic investigation in pursuit of ground water. For this purpose, 77 VES field stations were examined using the ABEM Terrameter SAS 4000 instrument (Sweden) and embellishments, such as hammer, stain less electrode and 30 meter tape to stimulate the localities for resistivity with depth in response to the electric field induced in the ground. The aquifer properties and susceptibility of aquifers to contaminants were analyzed by VES techniques upto 350 m spacing. The 4 electrodes (2 current +2 potential) were immersed in the ground. The current was introduced in current electrodes by means of cables and the resulting potential difference was measured with the assistance of potential electrodes. In Schlumberger arrangement, the spacing of electrodes from any particular distance of fixation was symmetrically increased for subsurface investigations with depth. The Geoelectric information was accessed upto 350 m spacing inside the Gujrat District (Fig. 1).

The acquired geo-electrical information were submitted to the iteration software IPI2WIN in order to inspect the information from 1D geo-electric measurements on solitary piece, automatically or semi-consequently and to get very precise results for extent, resistivity and profundity of underground stratum (Sultan et al., 2009).

The geo-electrical variables, such as, transverse resistance, conductance and anisotropy were figured out in a similar manner. Draft data were analyzed for the qualitative investigation of subsurface layers. In curve matching technique, the electrode spacing and apparent resistivity were plotted to accomplish the curve while the field curves were compared with master curves to acquire the results. So, the Geoelectric parameters were studied and qualitative observations of subsurface layer based on curve shapes were attained in curve matching technique. Earth can be divided into H, K, A and Q type of curves on the premise of shape. The underground layers are distributed as follows: H type,  $\rho_1 > \rho_2 < \rho_3$ ; K type:  $\rho_1 < \rho_2 > \rho_3$ ; A type:  $\rho_1 < \rho_2 < \rho_3$ ; Q type:  $\rho_1 > \rho_2 > \rho_3$ ;

KA, HQ type etc, thus demarcating the tetralogy of curves. Here  $\rho$  indicates the true resistivity of the layer.

The IPI2WIN software was used in the formulation of earth's resistivity model and computer software (surfer) was used in contour mapping. The values have been displayed at 2D contour maps. The iso-resistivity mapping was accomplished using Arc GIS 10.1 and Surfer version 9. Similarly the Rockworks version 2005 was used in modelling, interpreting the gauging the thickness of subsurface stratum.

### 4. Results and discussion

#### 4.1. Data interpretation

The quantitative interpretation of smooth curves (deduced through the set of data points) was made in curve matching technique (Fig. 2). Layer resistivity was calculated and the thickness was gauged from VES 1 to VES 77 (Table 2). The resistivity data interpretation has unveiled three to six layers at subsurface (Fig. 3). These layers form the lithological model which is the assemblages of clay, boulder clay, sandy clay, dry sandy soil, sand and gravels (Table, 2). The resistivity values falling in the range of 3005-5779 Ohm-m ( $\Omega$  m) in some locations indicate the presence of a sandstone bedrock. In addition, the low resistivity in the third and fourth layer has figured out ground water accumulation in the area. Moreover, the thickness of 20-270 m has been paced out for aquifers and the thickness exceeds in the Northeastern and Southwestern halves. Furthermore, the lithological model portrays subsurface geology through varying profiles (Fig. 4). However, the resistivity model of the study area has very close correspondence with the borehole data of well no 02, 05 and 07 (Fig. 5).

#### 4.2. Apparent resistivity

The iso-resistivity maps were compiled at different depths to delineate areas with variable ground water quality (Arulprakasam et al., 2014; Pal and Majumdar, 2001). The apparent resistivity values is in the range between 5-145  $\Omega$  m at 100 m, 200 m and 300 m depths and are illustrated on the respective contour maps

(Figs. 6a, 6b and 6c). In the map of 100 m electrode spacing (Fig. 6a) the highest resistivity (120 ohm-m) is observed in the north-east part of the area (Jalalpur Sobtian). The rest of the area is characterized by low values (30-55 ohm-m) of apparent resistivity pointing towards the groundwater potential in the area. In the map of 200 m and 300 m

electrode spacing (Figs. 6b & 6c) it was observed that the resistivity values generally decreased with increase in depth. The highest resistivity values (85 ohm-m) are observed in the Gujrat and surrounding area. The rest of the areas have low (35 ohm-m) resistivity values and demarcating good groundwater potential at these depths.

Table 2. Interpreted resistivity and subsurface geology of area

Sounding No.	Longitude E	Latitude N	Resistivity layers No.	Resistivity ( $\Omega$ m)	Lithology	Thickness (m)	Depth (m)
1	73°36.764E	33°03.022N	1	38	Clay	2.82	2.82
			2	10.4	Boulder clay	5.09	7.91
			3	63.9	Sand and Gravel	23.2	31.11
			4	7.8	Clay	47.5	78.61
			5	3005	Sandstone	--	--
2	73°35.741E	33°02.786N	1	52.3	Clay	1	1
			2	7.72	Gravel	5.2	6.2
			3	7.79	Boulder clay	9.23	15.43
			4	20	Siltstone	23	38.43
3	73°47.491	32°43.149	1	8.98	Clay	2.49	2.49
			2	5.9	Gravel	12.9	15.39
			3	6	Clay	23	38.39
			4	15.4	Boulder clay	57.2	95.59
			5	18.9	Siltstone	142	237.59
			6	12.2	Clay	--	--
4	73°45.543	32°40.776	1	177	Clayey Sand	1	1
			2	25.4	Boulder Clay	1.49	2.49
			3	25	Clay	3.71	6.2
			4	35	Boulder Clay	32.24	38.44
			5	35.5	Sandy Clay	200	238.44
			6	33.4	Clay	--	--
5	73°43.920	32°38.807	1	14	Clay	1	1
			2	14.7	Boulder Clay	1.49	2.49
			3	13.9	Clay	3.71	6.2
			4	14.5	Boulder Clay	9.23	15.43
			5	25.8	Sandy Clay	23	38.43
			6	18.9	Clay	--	--
6	73°46.571	32°37.648	1	15.3	Clay	15.4	15.4
			2	33.6	Sandy lay	23	38.4
			3	10	Clay	200	238.4
			4	466	Dry sandy Soil	--	--
7	73°49.053	32°37.486	1	10.1	Clay	1	1
			2	5.62	Clay	5.2	6.2

			3	5.2	Clay	17.1	23.3
			4	32.2	Boulder Clay	9.48	32.78
			5	35.5	Sandy Clay	200	232.78
			6	33.4	Clay	--	--
8	73°52.447	32°37.094	1	24	Clay	15.4	15.4
			2	12.8	Boulder Clay	223	238.4
			3	18.5	Sandy Clay	--	--
9	73°55.696	32°36.674	1	21.2	Clay	6.24	6.24
			2	117	Sandy clay	9.23	15.47
			3	10.3	Boulder Clay	80.9	96.37
			4	25.4	Clay	--	--
10	73°59.611	32°36.209	1	19.6	Clay	2.49	2.49
			2	24.8	Boulder Clay	12.9	15.39
			3	18.7	Sandy Clay	--	--
11	73°56.973	32°47.634	1	11.7	Clay	2.49	2.49
			2	10.4	Dry Clay	3.71	6.2
			3	17	Boulder Clay	9.23	15.43
			4	28.8	Sandy Clay	23	38.43
			5	25.3	Boulder Clay	57.2	95.63
			6	26.2	Clay	--	--
12	73°51.661	32°48.855	1	17.9	Clay	13.7	13.7
			2	57.2	Gravel	14.6	28.3
			3	21.2	Clay	--	--
13	73°49.421	32°50.639	1	457	Dry sandy clay	1.4	1.4
			2	104	Sandy Clay	8.05	9.45
			3	19.6	Boulder Clay	25.7	35.15
			4	49.8	Clay	--	--
14	73°47.359	32°53.068	1	503	Dry sandy soil	2.18	2.18
			2	217	Sandy clay	6.57	8.75
			3	14.4	Boulder clay	137	145.75
			4	1642	Gravel dry	--	--
15	73°42.370	32°54.660	1	19.3	Clay	3.68	3.68
			2	13.3	Boulder Clay	7.94	11.62
			3	129	Sandy clay	15	26.62
			4	17.9	Clay	--	--
16	73°49.373	32°55.443	1	39.3	Clay	2.49	2.49
			2	23.1	Boulder clay	35.9	38.39
			3	23.7	Sandy clay	57.2	95.59
			4	22.1	Boulder clay	142	237.59
			5	26.7	Clay	--	--
17	73°54.696	32°46.039	1	15.9	Clay	6.2	6.2
			2	25.5	Sandy clay	32.2	38.4
			3	12	Boulder clay	57.2	95.6

			4	24.8	Sandy clay	142	237.6
			5	1204	Gravel dry	--	--
18	73°56.278	32°46.549	1	25.7	clay	4.99	4.99
			2	11	Boulder clay	9.28	14.27
			3	79.6	Sandy clay	17.6	31.87
			4	12.6	Boulder clay	57.7	89.57
			5	46	Clay	--	--
19	73°57.747	32°47.659	1	853	Dry sandy soil	2.7	2.7
			2	215	Sandy clay	6.49	9.6
			3	23.2	Boulder Clay	--	--
20	74°00.652	33°47.264	1	35.7	Clay	15.4	15.4
			2	13	Boulder Clay	23	58.4
			3	40.7	Sandy Clay	57.2	115.6
			4	4.97	Clay	--	--
21	74°01.327	33°49.149	1	23.2	Clay	2.49	2.49
			2	29.2	Sandy Clay	12.9	15.39
			3	22.8	Boulder clay	223	238.39
			4	79	Clay	--	--
22	74°02.072	33°50.051	1	56.3	Clay	1.25	1.25
			2	12.8	Boulder Clay	11.4	12.65
			3	27.3	Sandy Clay	235	247.65
			4	825	Dry sandy Soil	--	--
23	73°53.014	32°55.306	1	52.4	Clay	3.16	3.16
			2	23.7	Sandy clay	49.7	52.86
			3	8.19	Boulder clay	119	171.86
			4	2687	Dry sandy soil	--	--
24	73°56.354	32°55.141	1	420	Dry Sandy soil	1	1
			2	132	Sandy Clay	5.2	6.2
			3	14	Boulder Clay	32.2	38.4
			4	20.4	Boulder clay	--	--
25	73°56.821	32°54.868	1	80.6	Clay	3.56	3.56
			2	37.4	Sandy clay	21.2	24.76
			3	16.4	Boulder Clay	49.2	73.96
			4	45.9	Sandy clay	102	175.96
			5	0.317	Clay	--	--
26	73°58.193	32°55.980	1	86.6	Clay	2.98	9.28
			2	39.5	Sandy Clay	8.03	85.98
			3	15.1	Boulder Clay	244	330
			4	415	Dry Sandy clay	--	--
27	74°00.452	32°56.037	1	110	Clay	20.9	44.5
			2	50.4	Sandy Clay	106	110.6
			3	15.5	Boulder Clay	--	--
28	73°56.472	32°43.055	1	123	Clay	2.79	4.59

			2	280	Dry Sandy Soil	14.2	16.99
			3	36.1	Boulder Clay	199	215.99
			4	10.7	Clay	--	--
29	74°03.679	32°52.524	1	75.4	Clay	6.21	6.21
			2	102	Sandy Clay	9.23	15.45
			3	24.3	Boulder Clay	223	238.45
			4	284	Dry Sandy Soil	--	--
30	74°02.589	32°54.508	1	62.8	Clay	15.4	15.4
			2	41	Sandy lay	223	238.45
			3	1481	Gravel Dry	--	--
31	74°00.966	32°55.377	1	246	Dry Sandy Soil	40.1	40.1
			2	15.1	Boulder Clay	58.9	99.0
			3	4496	Sandstone	--	--
32	74°01.239	32°53.769	1	106	Clay	10.4	10.4
			2	24.4	Boulder Clay	102	112.4
			3	3781	Sandstone	--	--
33	73°59.515	32°52.482	1	112	Clay	2.62	2.62
			2	89.7	Sandy Clay	9.31	11.93
			3	23.5	Boulder Clay	98.3	110.23
			4	4686	Sandstone	--	--
34	73°58.626	32°50.899	1	32.8	Clay	6.2	6.2
			2	14.8	Boulder Clay	32.2	38.4
			3	25.2	Sandy Clay	200	238.4
			4	5.75	Clay	--	--
35	73°44.031	32°53.532	1	24.6	Clay	3.8	3.8
			2	9.05	Boulder Clay	11.1	14.9
			3	97.1	Sandy Clay	11.1	26
			4	26.6	Clay	--	--
36	73°42.457	32°52.628	1	69.5	Clay	2.49	2.49
			2	32	Boulder Clay	35.9	38.39
			3	189	Sandy Clay	57.2	95.59
			4	0.271	Clay	--	--
37	73°40.027	32°50.472	1	192	Clay	95.9	95.9
			2	11	Boulder Clay	142	237.79
			3	9.11	Clay	--	--
38	73°38.417	32°48.025	1	35.7	Clay	6.2	6.2
			2	16.4	Boulder Clay	9.23	15.43
			3	542	Dry sandy Soil	23	38.43
			4	0.397	Clay	--	--
39	73°37.330	32°45.820	1	51.7	Clay	1	1
			2	309	Dry Sandy soil	5.21	6.21
			3	70	Sandy Clay	32.3	38.51
			4	255	Dry sandy soil	57.2	95.71

			5	1.02	Clay	--	--
40	73°36.196	32°44.108	1	33.8	Clay	11.9	11.9
			2	628	Dry sandy soil	24.4	36.3
			3	0.376	Clay	--	--
41	73°35.280	32°41.988	1	187	Dry Sandy soil	1.6	1.6
			2	159	Sandy clay	126	127.6
			3	38.9	Clay	--	--
42	73°35.762	32°40.966	1	70.2	Clay	6.2	6.2
			2	179	Sandy clay	9.23	15.43
			3	66.6	Clay	--	--
43	73°36.404	32°39.811	1	16.9	Clay	11.2	11.2
			2	41.7	Sandy clay	269	280.2
			3	712	Dry sandy soil	--	--
44	73°39.656	32°39.341	1	53	Clay	6.2	6.2
			2	32	Sandy Clay	6.2	12.2
			3	330	Dry Sandy soil	--	--
45	73°42.900	32°38.899	1	35	Clay	3.62	3.62
			2	7.77	Boulder Clay	8.7	12.32
			3	82.3	Sandy Clay	13.6	25.92
			4	12.3	Boulder Clay	51.1	77.02
			5	111	Clay	--	--
46	74°10.958E	32°37.777N	1	25.3	Clay	2.49	2.49
			2	45.5	Sandy Clay	3.71	6.2
			3	18.7	Boulder Clay	9.23	15.43
			4	29.5	Sandy clay	223	238.43
			5	11.5	Clay	--	--
47	74°09.468E	32°36.965N	1	92.4	Clay	1.17	1.17
			2	15.6	Boulder clay	19.4	20.57
			3	37.5	Sandy Clay	132	152.57
			4	922	Dry sandy soil	--	--
48	74°13.502E	32°39.687N	1	18.1	Clay	1.37	1.37
			2	858	Dry Sandy Soil	31.1	58.92
			3	35	Clay	--	--
49	74°15.150E	32°41.935N	1	53.8	Clay	6.2	6.2
			2	38.3	Boulder clay	9.23	15.43
			3	24.9	Sandy Clay	--	--
50	74°17.592E	32°43.693N	1	42.8	Clay	3.63	3.63
			2	12.3	Boulder Clay	10.3	13.93
			3	28.4	Sandy clay	42.5	55.95
			4	15.5	Boulder clay	216	271.95
			5	402	Dry Sandy soil	--	--
51	74°20.566E	32°43.280N	1	154	Clay	7.46	7.46
			2	582	Dry sandy soil	9.38	16.84

			3	49.5	Sandy Clay	--	--
52	74°22.275E	32°43.271N	1	81.7	Clay	1	1
			2	24.2	Gravels	0.862	1.86
			3	199	Sandy clay	5.25	7.11
			4	569	Dry sandy soil	8.61	15.7
			5	3.68	Gravel	25.7	40.8
			6	5779	Sandstone	--	--
53	74°24.113E	32°46.048N	1	60.7	Clay	3.2	3.2
			2	27.9	<b>Boulder clay</b>	11.8	15
			3	155	Sandy Clay	20.7	35.7
			4	66.3	Clay	--	--
54	74°05.458E	32°46.048N	1	45.9	Clay	1	1
			2	56.4	Sandy Clay	1.49	2.49
			3	25.7	Boulder clay	3.71	6.2
			4	21	Siltstone	9.23	15.43
			5	21.9	Boulder clay	223	238.43
			6	22.4	Clay	--	--
55	74°06.452E	32°39.086N	1	40.1	Clay	1	1
			2	22	Boulder clay	1.49	2.49
			3	5.59	Clay	3.71	6.2
			4	80.6	Sandy clay	9.23	15.43
			5	58.3	Gravel	23	38.43
			6	61	Clay	--	--
56	74°08.336E	32°40.887N	1	132	Clay	1	1
			2	128	Sandy Clay	1.49	2.49
			3	22	Boulder clay	12.9	15.39
			4	21.8	Clay	23	38.39
			5	21.9	Boulder Clay	57.2	95.59
			6	9137	Consolidated Shale	--	--
57	74°09.010E	32°41.375N	1	96.76	Clay	1	1
			2	33.99	Sandy Clay	1.489	2.489
			3	12.05	Boulder Clay	3.708	6.19
			4	46.06	Sandy clay	9.23	15.42
			5	19.32	Boulder Clay	80.33	95.75
			6	20.64	Clay	--	--
58	74°09.284E	32°42.967N	1	41.7	Clay	1	1
			2	40.5	Sandy clay	1.49	2.49
			3	43.1	Clay	3.71	6.2
				27.1	Sandy clay	9.23	15.44
				19.6	Boulder Clay	223	238.43
				21.2	Clay	--	--
59	74°10.604E	32°43.647N	1	61.2	Clay	1	1
			2	47.5	Sandy clay	1.49	2.49

			3	35.3	Boulder Clay	3.71	6.2
				37.5	Sandy Clay	9.23	15.44
				33.8	Boulder Clay	23	38.43
				26.6	Clay	--	--
60	74°12.855E	32°43.898N	1	18.4	Clay	2.49	2.49
			2	18.6	Boulder Clay	3.71	6.2
			3	28.8	Sandy Clay	9.23	15.44
			4	19.3	Siltstone	23	38.44
			5	18.2	Boulder clay	57.2	95.64
			6	18.2	Clay	--	--
61	74°17.543E	32°44.598N	1	201.1	Dry Sandy soil	1	1
			2	103.2	Clay	1.489	2.489
			3	27.27	Boulder clay	3.708	6.19
			4	44.24	Sandy clay	9.23	15.42
			5	30.59	Boulder clay	22.98	38.407
			6	26.86	Clay	--	--
62	74°04.745E	32°38.018N	1	48.6	Clay	2.49	2.49
			2	97	Dry Sandy soil	3.71	6.2
			3	147	Sandy clay	9.23	15.45
			4	35.4	Boulder Clay	23	38.45
			5	29.8	Sandy Clay	200	238.45
			6	13.7	Clay	--	--
63	74°04.990E	32°40.159N	1	222.7	Dry sandy soil	1	1
			2	178.8	Clay	1.489	2.489
			3	45.32	Sandy clay	3.708	6.19
			4	11.65	Boulder clay	9.23	15.42
			5	7.31	Gravel	80.19	95.91
			6	7.82	Clay	--	--
64	74°04.695E	32°41.362N	1	5.06	Clay	1	1
			2	4.77	Dry Soil	1.49	2.49
			3	5.11	Clay	3.71	6.2
			4	11.2	Boulder clay	9.23	15.43
			5	7.23	Gravel	80.2	95.63
			6	10.1	Clay	--	--
65	74°04.428E	32°42.885N	1	9.88	Clay	4.66	4.66
			2	7.46	Gravel	10.8	15.46
			3	57.2	Dry Sandy soil	11.8	27.26
			4	17.6	Clay	--	--
66	74°04.310E	32°44.305N	1	45.8	Clay	3.64	3.64
			2	74.2	Sandy Clay	6.46	10.1
			3	16.8	Boulder clay	--	--
67	74°03.933E	32°47.073N	1	25.6	Clay	3.96	3.96
			2	16.5	Boulder Clay	41.2	45.16

			3	38.5	Sandy Clay	--	--
68	74°03.937E	32°50.241N	1	20.5	Clay	1	1
			2	21	Siltstone	5.2	6.2
			3	20.7	Boulder Clay	32.2	38.4
			4	20.5	Siltstone	57.2	95.6
			5	21.8	Boulder Clay	142	237.6
			6	91.4	Clay	--	--
69	74°04.441E	32°52.811N	1	31.4	Clay	2.49	2.49
			2	13.8	Dry Clay	3.71	6.2
			3	14.5	Boulder Clay	9.23	15.43
			4	24.2	Sandy clay	23	38.43
			5	23.6	Boulder Clay	200	238.43
			6	11.8	Clay	--	--
70	74°05.320E	32°50.807N	1	176	Clay	8.2	8.2
			2	93.3	Sandy Clay	3.97	11.99
			3	20.3	Boulder Clay	--	--
71	74°08.620E	32°49.427N	1	32.7	Clay	3.51	3.51
			2	36.2	Boulder Clay	128	131.51
			3	19	Clay	--	--
72	74°10.790E	32°47.676N	1	82	Clay	3.82	3.82
			2	218	Sandy clay	8.45	12.27
			3	36.6	Boulder Clay	105	117.27
			4	28.8	Clay	--	--
73	74°14.991E	32°45.598N	1	42.8	Clay	2.49	2.49
			2	13.8	Boulder Clay	13	15.49
			3	27.7	Sandy clay	23	38.49
			4	6.13	Gravel	57.2	95.69
			5	45.8	Clay	--	--
74	74°01.385E	32°32.828N	1	30.5	Clay	2.49	2.49
			2	14.9	Boulder Clay	12.9	15.39
			3	33.2	Sandy clay	23	38.39
			4	17	Boulder Clay	200	238.39
				366	Dry sandy Soil	--	--
75	74°00.757E	32°31.255N	1	37.4	Clay	2.49	2.49
			2	62.5	Sandy clay	3.71	6.2
			3	27.4	Boulder Clay	32.2	38.4
			4	39.9	Sandy clay	--	--
76	73°59.636E	32°32.304N	1	29.4	Clay	2.49	2.49
			2	131	Sandy Clay	3.71	6.2
			3	29	Boulder clay	32.2	38.4
			4	41.4	Sandy clay	--	--
77	73°56.227E	32°30.979N	1	4.76	Clay	3.11	3.11
			2	2.67	Gravel	6.59	9.6
			3	159	Sandy clay	14.3	23.9
			4	4.84	Gravel	52.7	76.6
			5	1250	Dry sandy soil	--	--

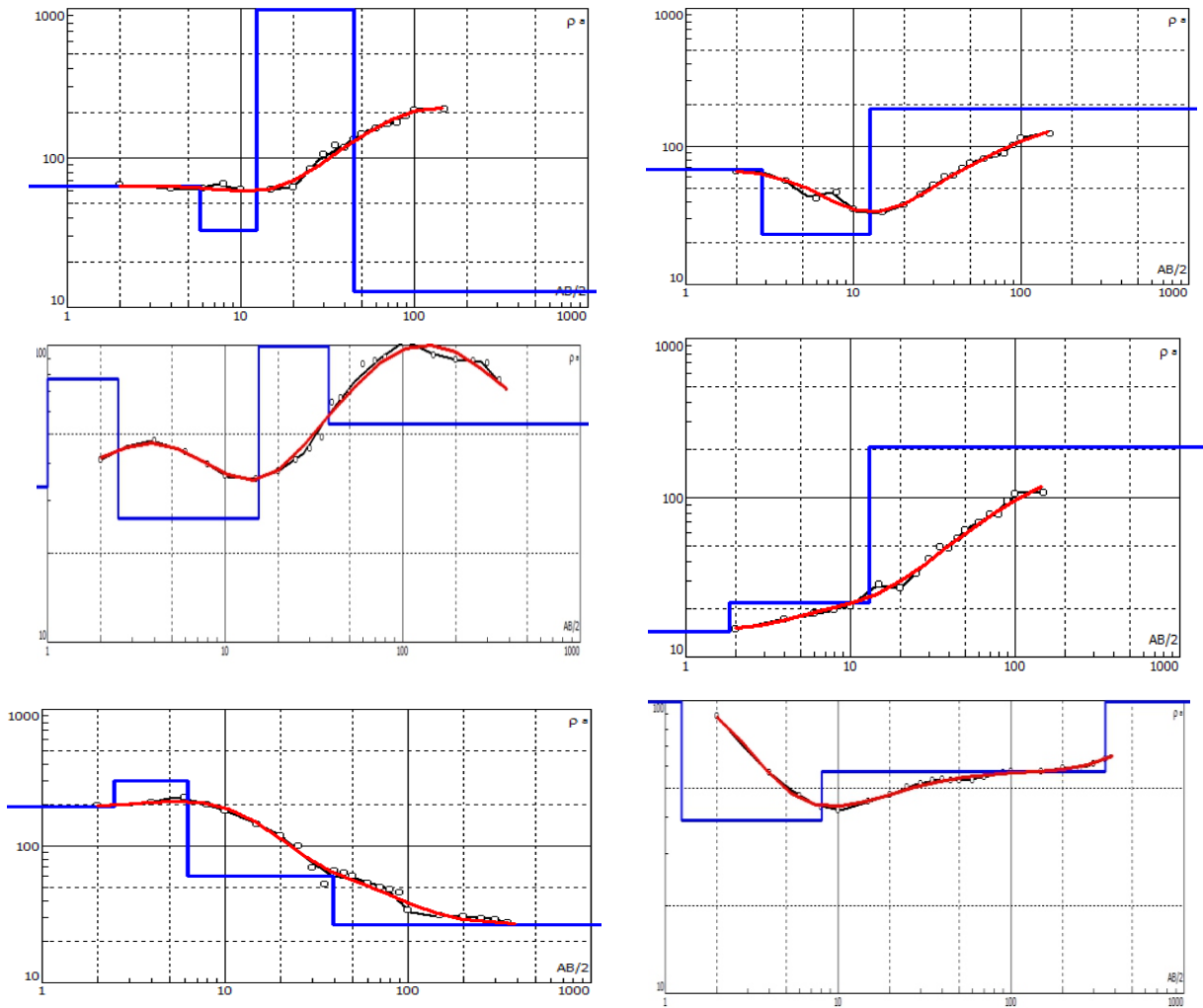


Fig. 2. Typical four layered VES curves.

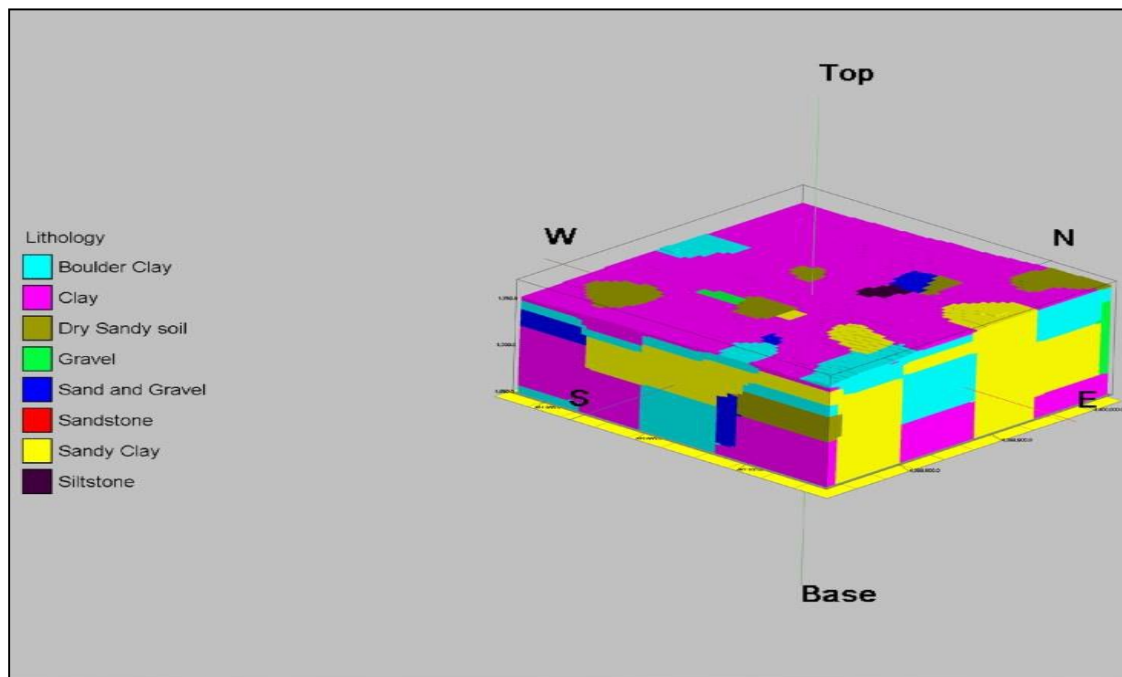


Fig. 3. Geological model computed on the basis of resistivity data of Gujrat.

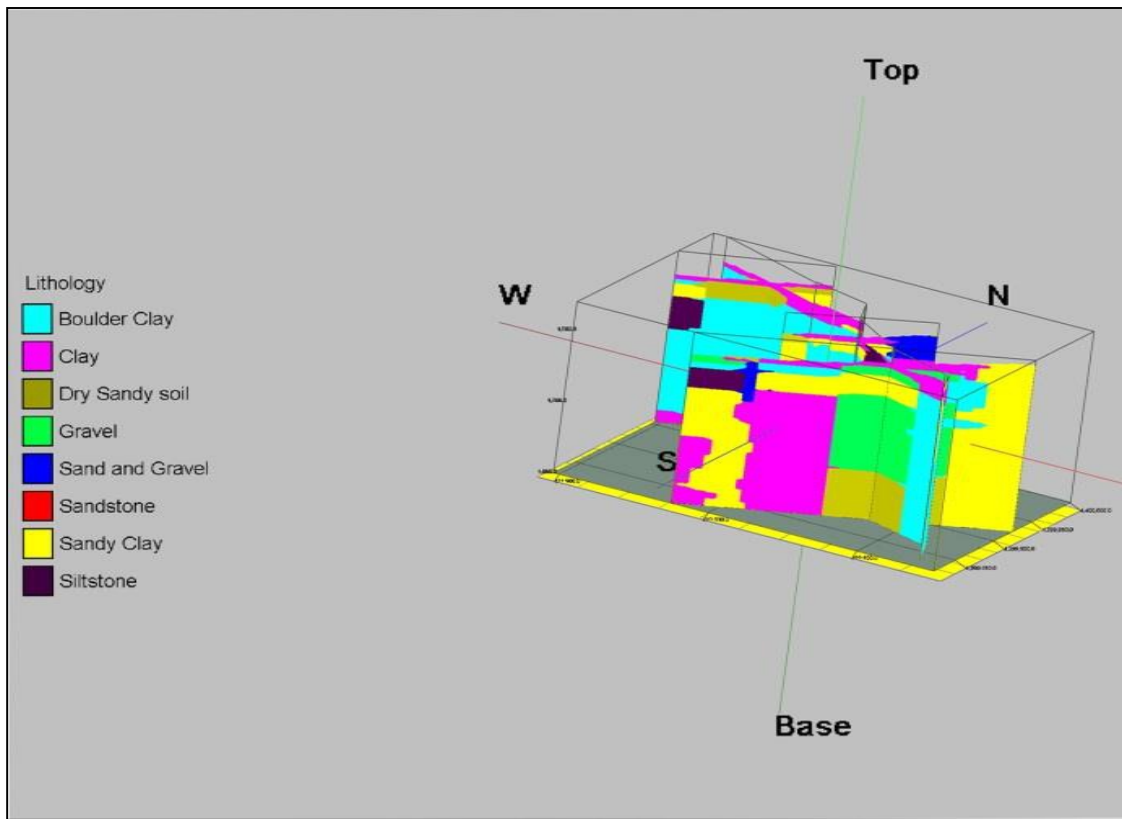


Fig. 4. Lithological fence diagram of Gujrat.

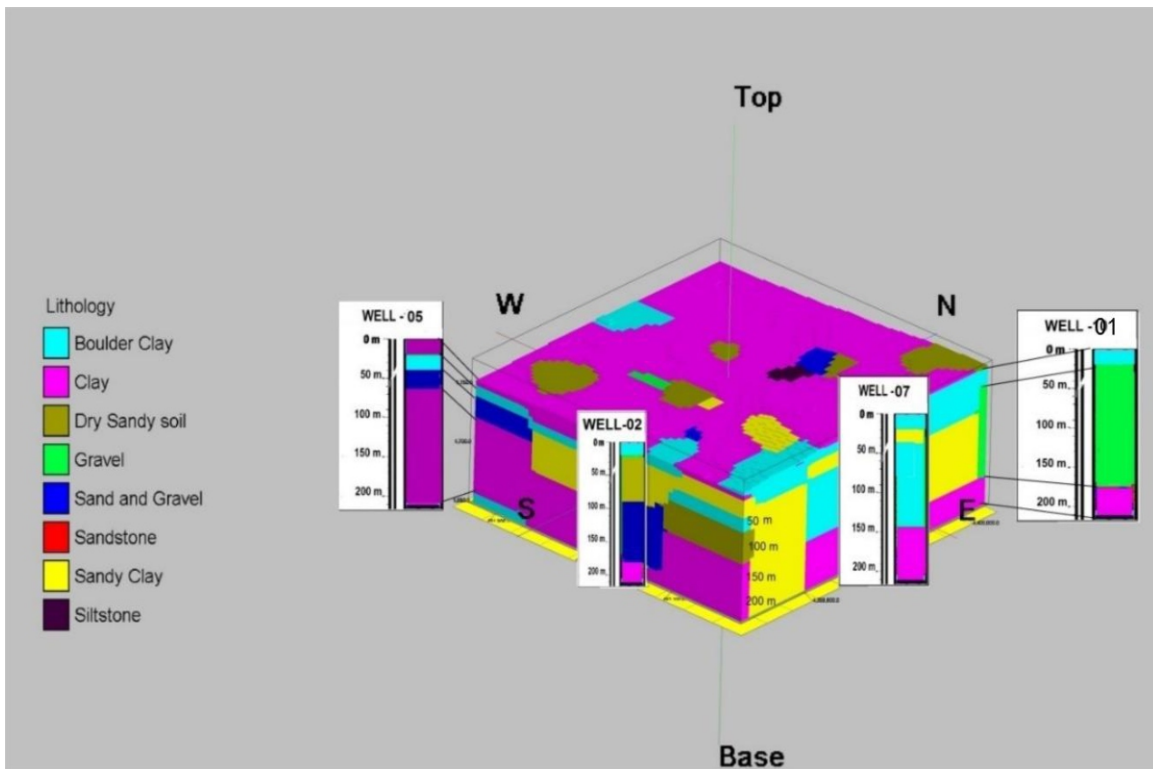


Fig. 5. Correlation of resistivity model and borehole data of Gujrat.

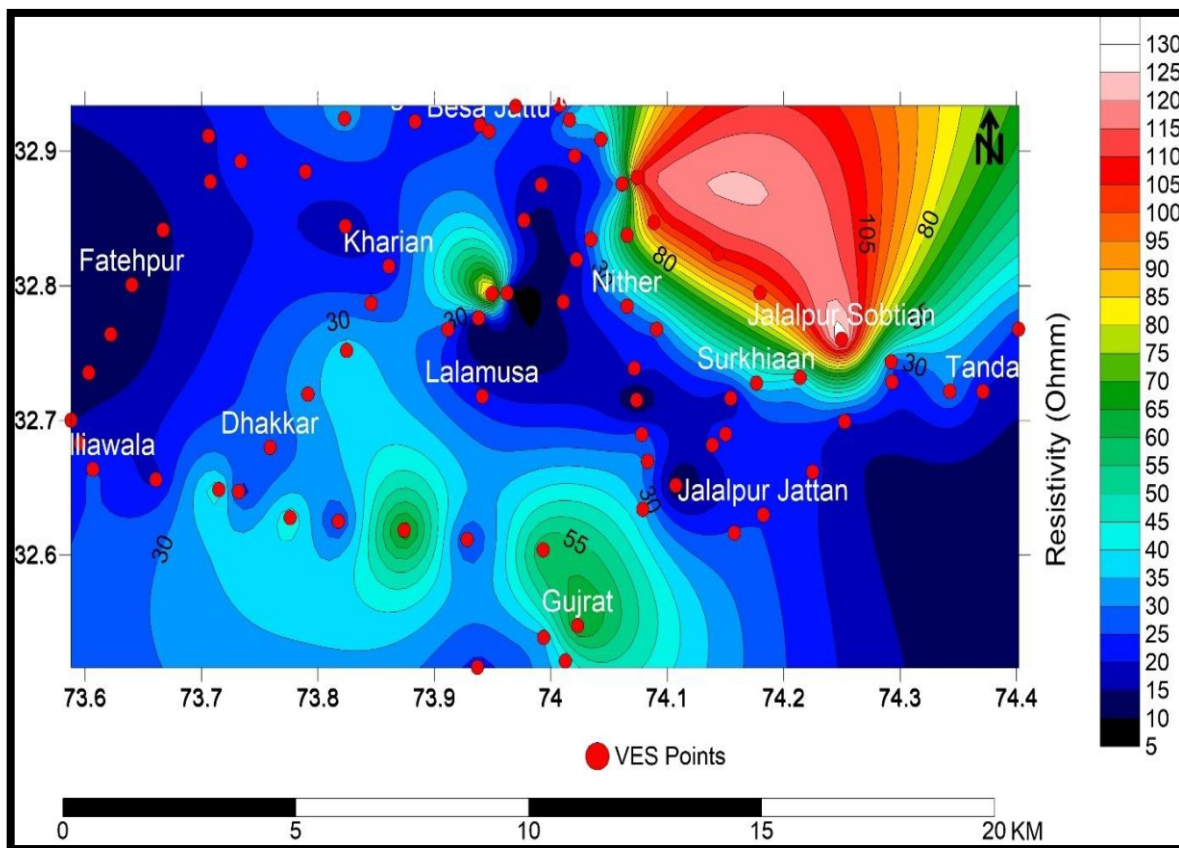


Fig. 6 (a). Apparent resistivity contour map of Gujrat at 100 m spacing.

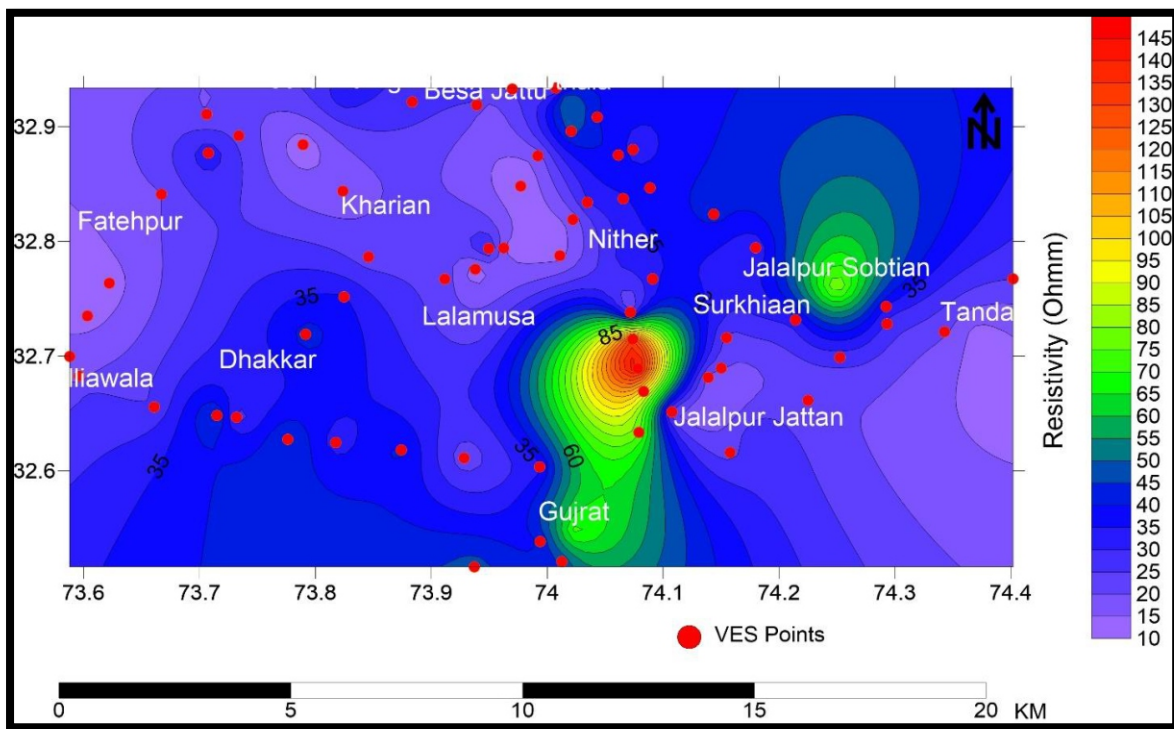


Fig. 6 (b). Apparent resistivity contour map of Gujrat at 200 m spacing.

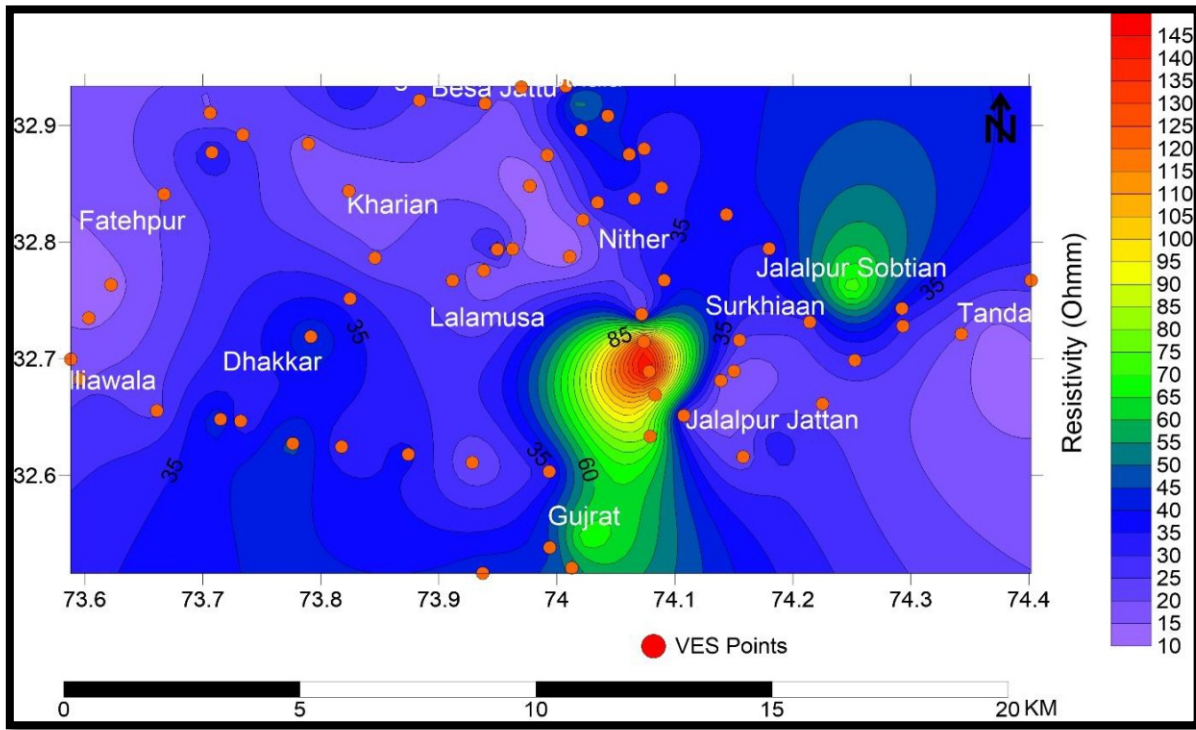


Fig. 6 (c). Apparent resistivity contour map of Gujrat at 300 m spacing.

#### 4.3. Longitudinal conductance

Longitudinal conductance refers to the transmission of current in the bedding plane direction through a 1m column. It is represented by the letter S (in  $\Omega$ ) (Nwanko et al., 2011; Parasnis 1979).

$$S = h_1 / \rho_1 = h_2 / \rho_2$$

$$S = \sum_{i=1}^n h_i / \rho_i$$

Where, h indicates the layer thickness,  $\rho$  denotes the layer resistivity while the prodigious S values commonly represent the thick successions and are known for giant primacy in evaluating subsurface water potential (Slater, 2007).

Total longitudinal conductance contour map is displayed in Figure 7. The conductance values fall between 0 to 22 Siemen. The values are high in northwestern (Fatehpur area) and central part (Lalamusa & Dhakkar area) of the study area. The vulnerability map compiled by the unit longitudinal conductance exhibits the distributive trend of overburden protection of the aquifers in the project region (Fig. 7).

Based on this rating the study area has been grouped in terms of protective capacity zones (Table 1). The aquifer vulnerability map delineates the impermeability of overburden clay layer. Values  $< 0$  mhos show poor to weak protective capacity zone with risk of defilements, while 0-5 mhos demonstrates good protective zones.

#### 4.4. Transverse resistance

The longitudinal conductance determines the characteristics of conducting layers as compared to the transverse resistance showing the characteristics of resistive layers (Yungul, 1996). It is defined in terms of total resistance numerated through 1 m column orthogonal to plane. It is symbolized by T (in  $\Omega$  m-1) (Nwanko et al., 2011; Parasnis 1979):

$$T = h\rho_1 + h\rho_2 + \dots + h\rho_n$$

$$T = \sum_{i=1}^N h_i \rho_i$$

$$T = \sum_{i=1}^N T_i$$

Where  $h$  and  $\rho$  indicates thickness and true resistivity respectively and  $N$  indicates the quota of layers in the portion.  $T$  forms direct relationship to the transmissivity and prodigious  $T$  values narrate higher transmissivity values of aquifer respectively. Most part of the study area has low resistivity

values of 100-150 ohm m (Fig. 8) having groundwater potential. These values are compatible with the presence of ground water in the area. The two closures with high resistivity in Kharian and Nither area have been identified. Hence this area is devoid of ground water potential.

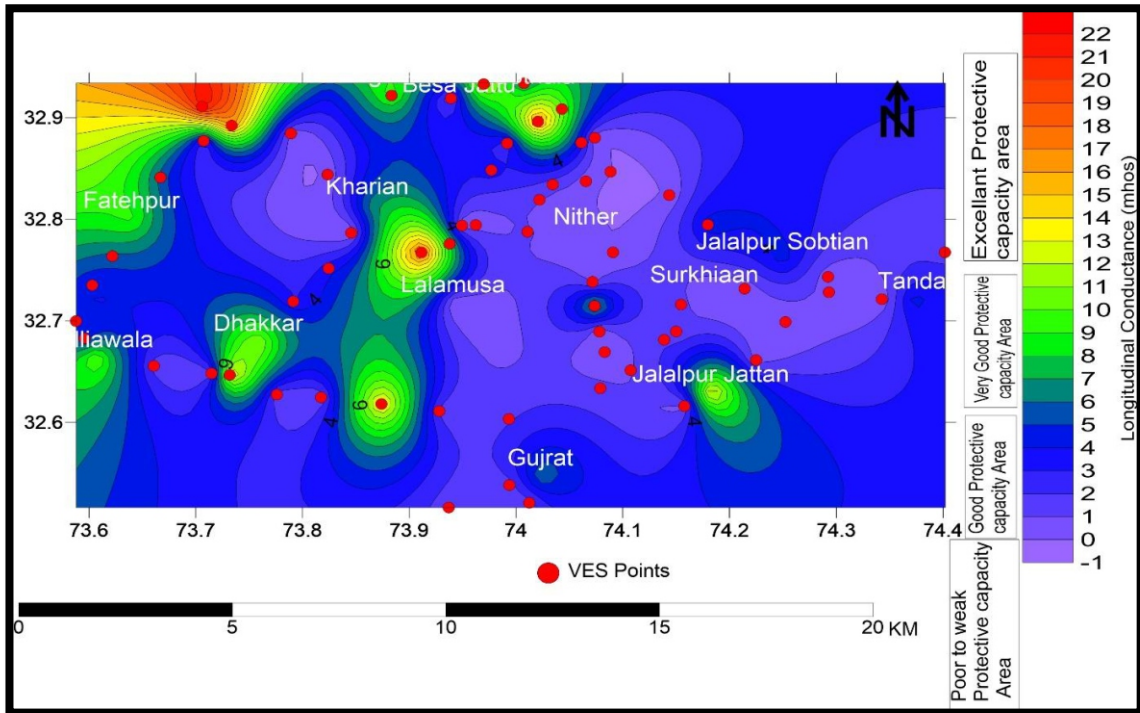


Fig. 7. Longitudinal conductance map of Gujrat.

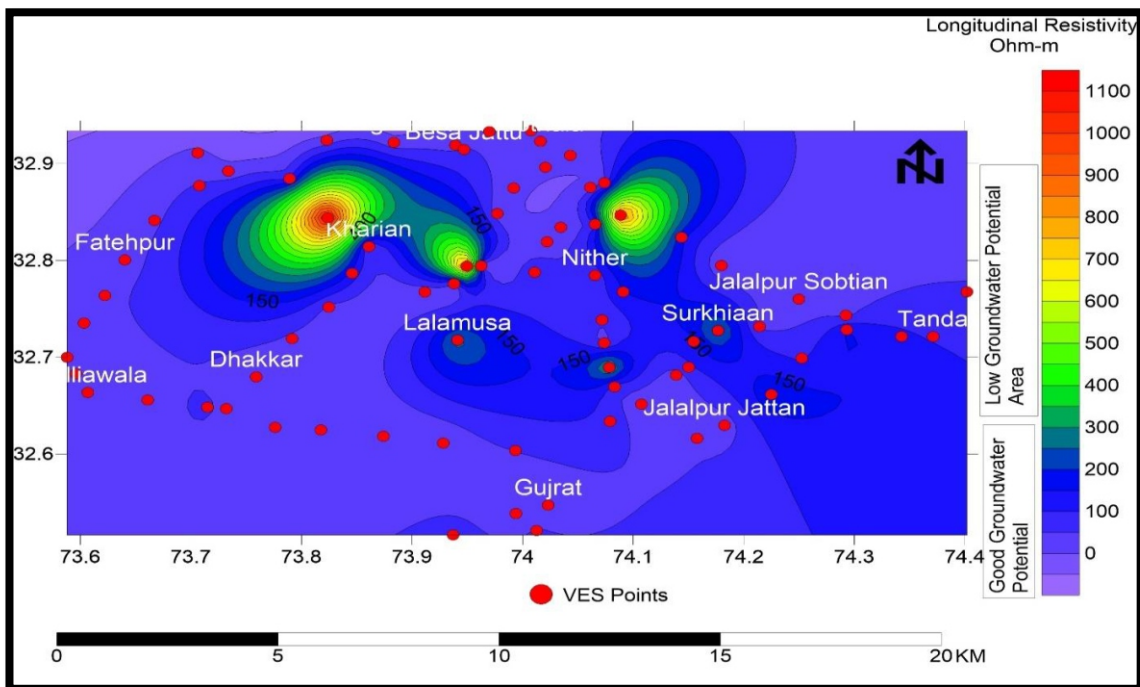


Fig. 8. Longitudinal resistivity map of Gujrat area.

The Figure 9 most parts with low resistivity values (0-150 ohm m) and indicates ground water assemblage in the area. The southeastern part and Nither area have closures with high resistivity indicate least potential or absence of potential of ground water.

The Figure 10 illustrates the coefficient of anisotropy ( $\lambda$ ). The value fluctuates in the range of 0 to 5. The Nither area and southeastern half of the area is known for high values as compared to the remaining halves with low coefficient of anisotropy. The low anisotropy and

high isotropy in the most part of the study area indicates weak protection against pollution and shows a high susceptibility for the contaminants. The ground water may be contaminated by polluted fluids leached in this area from dump sites as well as from sewage lines. The south-eastern and Nither area is characterized by “Good” protective area for infiltration of fluids. The chemical analysis results also delineated good quality drinking water in the wells number 01, 07 & 03 from this area.

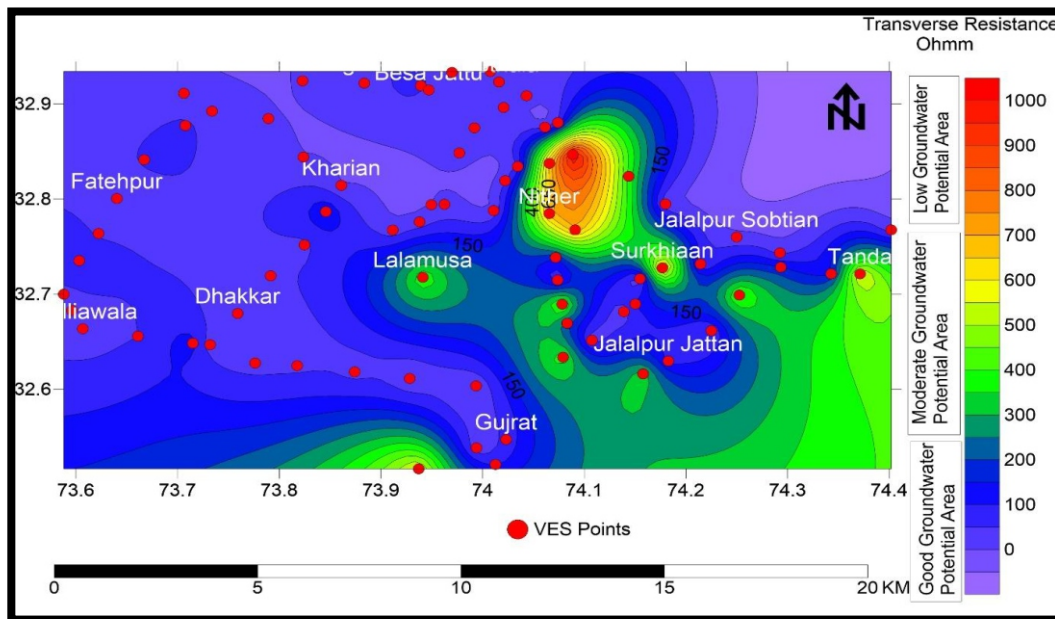


Fig. 9. Transverse resistance map of Gujrat area.

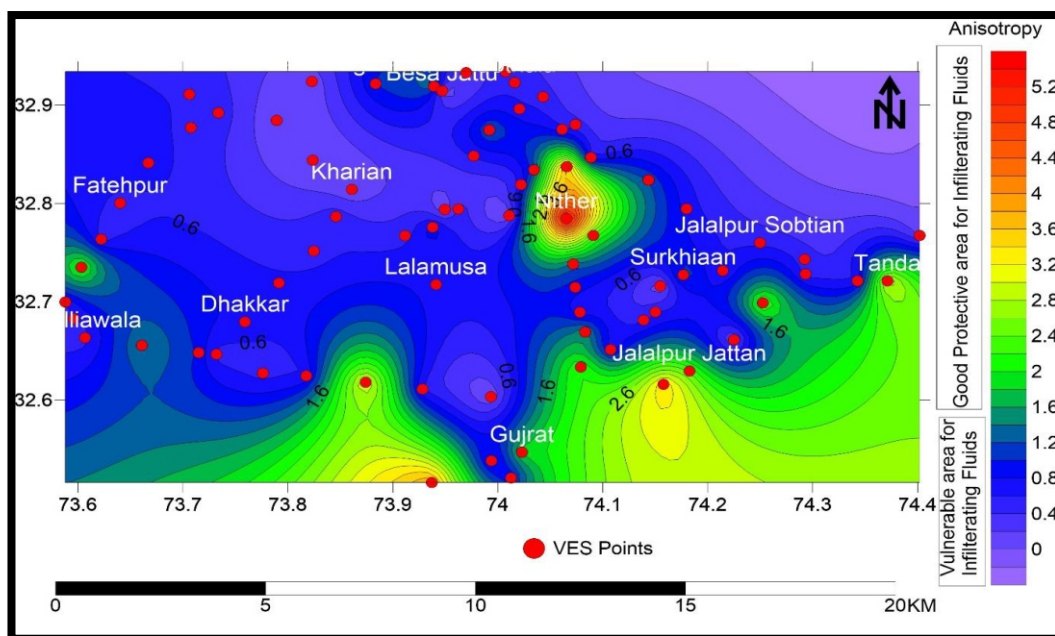


Fig. 10. Anisotropy map of Gujrat area.

#### 4.5. Chemical analysis

To carryout chemical analysis the water was sampled from eight different wells in the research area (Fig. 1). Monographic studies have been numerated under table 3. The results indicate that the hardness of water is high as compared to World Health Organization WHO limit (500 mg/L) in sample number 2, 4, 5 and 6 are 562, 670, 534 and 598 mg/L respectively. The nitrates concentration (14 mg/L) is also found high in sample number 1 and 3 than WHO limit (10 mg/L). The sample number 5

(425 mg/L) and 6 (488 mg/L) are found concentrated with chloride salts than WHO limit (250 mg/L). The potassium concentration is also higher than WHO limit in sample 4 (1 mg/L), 5 (1.5 mg/L), 6(1.4 mg/L) and 7 (1.3 mg/L) than WHO defined limit (0.4 mg/L). The water in this portion of the area from wells (02, 04, 05 & 06) is found unsafe for drinking. The Total Dissolved Salts (TDS values were observed less than 1000 mg/L WHO limit in most of samples.

Table 3. Results of chemical analysis of water samples from Gujrat.

Parameters	Sam ple # 1	Sample # 2	Sample # 3	Sample # 4	Sample # 5	Sample # 6	Sample # 7	Sample # 8	WHO/ PSQC A Limit
E.C (µs/cm)	3200	1764	1689	1210	3490	1050	722	1145	NGVS
pH	7.40	7.77	7.47	7.43	7.19	7.42	7.22	7.31	6.5-8.5
Turbidity (NTU)	4.59	3.93	3.65	3.44	1.49	BDL	0.7	3.63	Less than 5NTU
Alkalinity (mg/L)	360	258	331	357	312	319	488	323	NGVS
Bicarbonate (mg/L)	313	381	492	353	287	302	312	387	NGVS
Calcium (mg/L)	145	135	187	175	397	345	220	210	NGVS
Carbonate mg/L	BDL	BDL	BDL	BDL	BDL	BDL	BDL	BDL	NGVS
Chloride (mg/L)	88	60	88	130	425	488	220	110	250
Hardness (mg/L)	490	562	377	670	534	598	470	490	500
Magnesium (mg/L)	44	32	72	64	88	170	76	59	NGVS
Nitrate (mg/L)	14	9	14	10	10	9	4	7	10
Potassium (mg/L)	0.4	0.4	0.4	1	1.5	1.4	1.3	0.4	0.4
Sodium (mg/L)	66	24	77	120	88	83	190	110	NGVS
Sulphate mg/L	120	90	110	120	110	120	130	156	NGVS
TDS (mg/L)	755	517	876	889	890	970	950	816	1000
Lead (µg/L)	BDL	BDL	BDL	BDL	BDL	BDL	BDL	BDL	50
Arsenic (µg/L)	0.34	1.47	0.10	1.83	30.0	BDL	BDL	1.23	50

NGVS: no Guideline value set, WHO: World Health Organization, PSQSA: Pakistan standard quality control authority, BDL: Below detection limit, ppm: Parts per million

#### 4.6. Aquifer unit(s) thickness map

The aquifer thickness map in a phase of conation is peculiar to geological formations in compiling entire area as one of the good, moderate and poor potential zones of subsurface water and symbolic of the estimated volume of water at every VES station akin to

the respective aquifer thickness. The aquifer thickness map of the project area is shown in Figure 11. The thickness of about 20-210 m for aquifers was gauged in the study area. The area straddles moderate to good ground water potential zones. The peak in the Figure 12 is harbinger of good subsurface water potential.

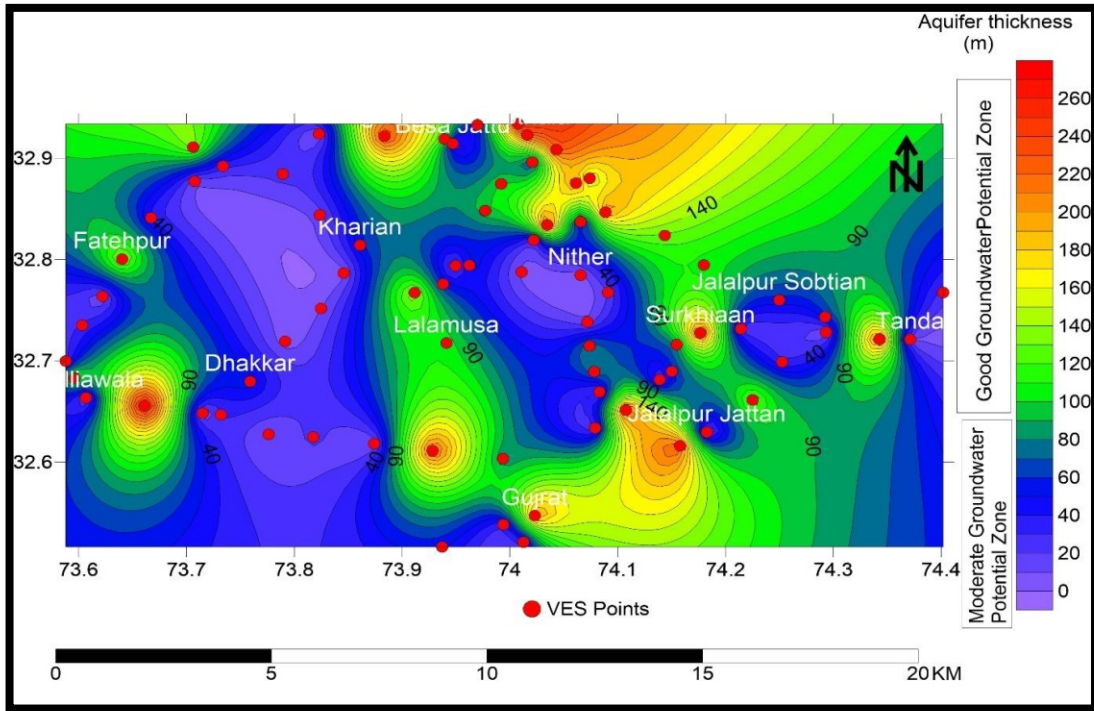


Fig. 11. Aquifer thickness Gujrat area.

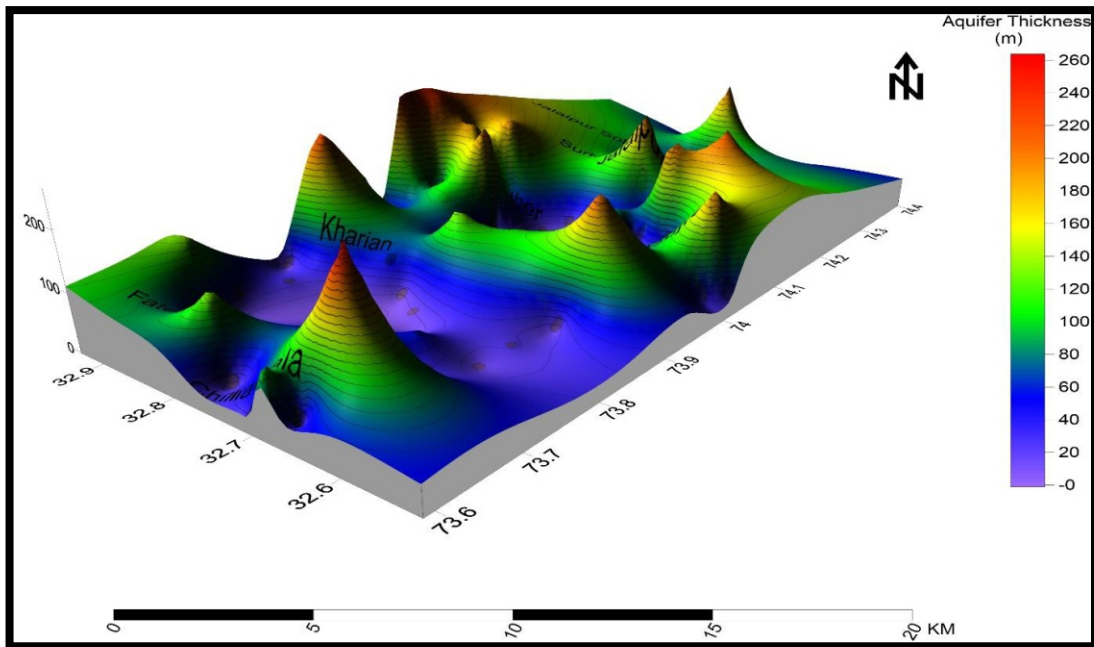


Fig. 12. 3D map of aquifer thickness Gujrat.

#### 4. Conclusion

The present study delineates thickness and lithologies of subsurface layers by using geoelectric method. The presence of potential ground water regions are marked on the basis of geo-electrical data and are represented mostly by H type curves. The southern, northeastern and western part of the study area is characterized by good productive ground water zones. The third and fourth layers indicate the presence of water bearing strata with low resistivity values. The VES at points 1, 31, 32, 33 and 52 indicate fifth layer of compact sandstone with resistivity values range between 3005 to 5779 ohm-m. The comparison between borehole stratigraphy data and the geophysical investigations confirms the presence of sandstone. The study allowed to understand that future wells need to be drilled within third and fourth water bearing layer detected in different regions. The existence of broad aquiferous region (20-210m) assures the area of good drinking water resources. The aquifer vulnerability map delineates the impermeability of overburden clay layer. Values  $< 0$  mhos show poor to weak protective capacity zone with risk of defilements, while 0-5 mhos demonstrates good protective zones. The outcomes were additionally checked by anisotropy mapping and chemical investigation of water samples of the study area. The outcomes of anisotropy values show that Nither area and southern halves of the area is characterized by good protective for fluid infiltration while remaining area is vulnerable for infiltrating fluids. The water from this area is found polluted with chlorides, nitrates and sulphates salts.

#### *Authors' Contribution*

*Abrar Niaz, proposed the main concept and Idea about the research work and also involved in field work supervision. Muhammad Rustam khan supervised whole project from planning, data acquisition, processing and interpretation. Fahad Hameed did provision of relevant literature, Aamir Asghar did technical review before submission and proof read of the manuscript, Umair Bin Nisar, involved in review and proof read of the manuscript in write up. Jawad Niaz involved in the data acquisition in field, Muhammad Farooq developed the maps on GIS, Muhammad Yasin khan was involved in data acquisition and surface geological map*

*development, Mansoor Awan was also involved in data acquisition process and preparation of illustration and plates of figures.*

#### References

- Adeoti, L., Alile, O. M., Uchegbulam, O., Adegbol, R. B., 2012. Geoelectrical investigation of groundwater potential in Mowe, Ogun state, Nigeria. *British Journal of Applied Science & Technology*, 2(1), 58-71.
- Ako, A. O., Olorunfemi, M. O., 1989. Geoelectric survey for groundwater in the newer basalts of Vom Plateau Satae, Nigeria. *Journal of Mining Geology*, 25 (1&2), 247-450.
- Arulprakasam, R., Siva, K., Gowtham, B., 2014. Electrical Resistivity Technique for Demarcation of Groundwater Quality Zones in Parts of Vanur block, Villupuram District, Tamil. *International Journal of Geology, Agriculture and Environmental Science*, 2(1), 28-30.
- Anomohanran, O., 2013. Geoelectrical investigation of groundwater condition in Oleh, Nigeria. *International Journal of Research and Reviews in Applied Sciences*, 15(1), 145-151.
- Awni, T. B., 2010. Mapping Quaternary deposits in the el-Jufr playa (Southeastern Jordan Plateau) using geoelectrical techniques: Implications for geology and hydrogeology. *Scientific Research and Essays*, 5(20), 3183-3192.
- Bayewu, O. O., Oloruntola, M. O., Mosuro. G., 2014. Evaluation of resistivity anisotropy of parts of ijebu Igbo, Southwestern, Nigeria Using Azimuthal Resistivity Survey (ARS) Method. *Journal of Geography and Geology*, 6(4), 140-152.
- El-Qady, G., 2006. Exploration of a geothermal reservoir using geoelectrical resistivity inversion case study at Hammam Mousea, Sinai, Egypt. Case study at hummammoousesiniai, Egypt. *Journal of Geophysics and Engineering*, 3, 114-121.
- Ekwe, A. C., Onuoha, K. M. Ugwumbah K. I., Onwuka., O. S., 2010. Estimation of aquifer hydraulic characteristics of low permeability formation from geosounding data: the case of O d u m a town Enugu state. *Journal of Earth Science*, 4(1), 19-26.

- Gowd, S. S., 2004. Electrical resistivity survey to delineate the ground water potential aquifers in Peddavanka watershed, Anantapur District, Andhra Pradesh. *The journal of environmental geology*, 46, 118-131.
- Henriet, J. P., 1976. Direct application of the Dar Zarrouk parameters in groundwater surveys. *Geophysical Prospecting*, 24, 344-353.
- Kalisperi, D., Soupios, P., Kouli, M., Barsukov, P., Kershaw, S., Collins, P., Vallianatos, F., 2009. Coastal aquifer assessment using geophysical methods (TEM, VES), case study: Northern Crete, Greece, 3rd IASME/WSEAS international conference on geology and seismology (GES'09) Cambridge, UK, 24-26.
- Kemna, A., Vanderborght, J., Kulesa, B., Veerecken, H., 2002. Imaging and characterization of subsurface solute transport using electrical resistivity tomography (ERT) and equivalent transport model, *Journal of Hydrology*, 267, 125-146.
- Kelly, W. E., Stanesly, M., 1993. *Applied geophysics in hydrogeological and engineering practice*. Practice. Elsevier, Amsterdam, 292.
- Kenneth, S. O., Edirin, A., 2012. Determination of aquifer properties and groundwater vulnerability mapping using geoelectric method in Yenagoa city and its Environs in Bayelsa state, south Nigeria. *Journal of Water Resource and Protection*, 4 (2), 354-362.
- Madan, K. J., Kumar, S., Choudry, A., 2008. Vertical electrical sounding survey and resistivity inversion using genetic algorithm optimization technique. *Journal of Hydrology*, (359), 71-87.
- Niaz, A., Khan, M. R., Ijaz, U., Yasin, M., Hameed, F., 2018. Determination of groundwater potential by using geoelectrical method and petrographic analysis in Rawalakot and adjacent areas of Azad Kashmir, sub-Himalayas, Pakistan. *Arabian Journal of Geoscience*, 11, 468 <https://doi.org/10.1007/s12517-018-3811-0>.
- Niaz, A., Khan, M. R., Asghar, A., Mustafa, S., Hameed, F., Umair, B. N., Khan, S., Mughal, M. S., Farooq, M., Rizwan, M., 2017. The study of aquifers potential and contamination based on geoelectric technique and chemical analysis in Mirpur Azad Jammu and Kashmir, Pakistan. *Journal of Himalayan Earth Sciences*, 50 (2), 60-73.
- Niaz, A., Khan, M. R., Asghar, A., Mustafa, S., Hameed, F., 2013. Determination of groundwater potential in Mirpur Azad Jammu and Kashmir, Pakistan using geoelectric method vertical electrical sounding. *International Journal of Scientific & Engineering Research*, 4, 2229-5518.
- Nisar, B. U., Khan, M. R., Khan, S., Farooq, M., Rizwan, M., Ahmed, K. A., Razzaq, S. S., Niaz, A., (2018). Quaternary Paleodepositional Environments in relation to Ground water occurrence in lesser Himalayan Region, Pakistan. *Journal of Himalayan Earth Sciences*, 51(1), 99-112.
- Nwanko, C., Nwasu, L., Emujakporue, G., 2011. Determination of Dar Zarouk parameters for a s s e s s m e n t o f groundwater potential: case study of Imo State, Southeastern Nigeria. *International Journal of Innovation and Sustainable Development*, 2(8), 57-71.
- Ogunbe, A. S., Onori, E. O., Olaoye. M. A., 2012. Application of electrical resistivity techniques in the investigation of groundwater contamination: A case study of Ile-Epo, dumpsite Lagos, Nigeria. *International Journal of Geomatics and Geosciences*, 3(1), 117-123.
- Olorunfemi, M. O., Meshida, E. A., 1989. *Engineering geophysics and its application in engineering site investigation*. Nigerian Engineer, 22(2), 57-66.
- Olowofela, J. A., Jolaosho, V. O., Bandmus, B. S., 2005. Measuring the electrical resistivity of the earth using a fabricated resistivity meter. *European Journal of Physics*, 26, 501-515.
- Omosuyi, G., Adeyemo O., Adegoke, A. O., 2007. Investigation of groundwater prospect using geoelectric and electromagnetic sounding at Afunbiowo near Akurea Southwestern Nigeria. *The Pacific Journal of Science and Technology*, 8(1), 172-182.
- Oseji, J. O., Atakpo, E. A., Okolie, E.C., 2005.

- Geoelectric investigation of the aquifer characteristics and groundwater potential in Kwale, Delta state, Nigeria. *Journal of Applied Sciences and Environmental Management*, 9, 157-160.
- Pal, S. K., Majumdar, R. K., 2001. Determination for groundwater potential zones using Iso-resistivity map in the alluvial areas of Munger District, Bihar. *Journal of Earth Science*, (1-4), 16-26.
- Parasnis, D. S., 1979. *Principle of applied geophysics*, third edition, Chapman and Hall, London: 275.
- Shah, S. M. I., 2009. Stratigraphy of Pakistan. *Memoirs of the Geological Survey of Pakistan*, 22, 293-298.
- Shah, S. M. I. 1977. Stratigraphy of Pakistan. *Mem. Geological Survey of Pakistan*, 12, 137.
- Slater L., 2007. Near surface electrical characterization of hydraulic conductivity from petrophysical properties to aquifer geometries. *Revised Surveys in Geophysics*, 28, 167-169.
- Stanley, N. D., DeWiest, J. M., 1996. *Hydrogeology*, John Wiley Sons New York: 280-286.
- Soupios, P., Kouli, M., Vallianatos, F., Vafidis, A., Stavroulakis, G., 2007. Estimation of aquifer parameters from surficial geophysical methods. A case study of Keritis Basin in Crete. *Journal of Hydrology*, 338, 122-131.
- Stampolidis A., Tsourlos, P., Soupios, P., Mimides, T.H., Tsokas, G., Vargemezis, G., Vafidis, A., 2005. Integrated geophysical investigation around the brackish spring of Rina, Kalimnos Isl., SW Greece. *Journal of Balk Geophysical Society*, 8(3), 63-73.
- Sultan, S. A., Mekhemer, H. M., Santos, F. A., Abdulla, M., 2009. Geophysical measurement for subsurface mapping and groundwater exploration at the central part of Sinai Peninsula, Egypt. *The Arabian Journal for Science and Engineering*, 34(1A), 103-119.
- Vanderborght, J., Kemna, A., Hardelauf, H., Vereecken, H., 2005. Potential of electrical resistivity tomography to infer aquifer transport characteristics from tracer studies: a synthetic case study, *Water Resources Research*, 41. Wo06013, doi:10.1029/2004WR003774. [www.en.climate-data.org.pk](http://www.en.climate-data.org.pk).
- Yungul, S. H., 1996. Electrical methods in geophysical exploration of sedimentary basin. Chapman and Hill, U.K, 152.
- Zohdy, A., Eaton, G., Mabey, D., 1974. Application of surface geophysics to groundwater investigations. *Techniques of Water-Resources Investigation of the United States Geological Survey*, 2, 116-119.